

Lifetime of dynamic heterogeneity in strong and fragile kinetically constrained spin models

Sebastien Leonard and Ludovic Berthier^z

Laboratoire des Colloïdes, Verres et Nanomatériaux, UMR 5587 CNRS and
Université Montpellier II, 34095 Montpellier Cedex 5, France

Abstract. Kinetically constrained spin models are schematic coarse-grained models for the glass transition which represent an efficient theoretical tool to study detailed spatio-temporal aspects of dynamic heterogeneity in supercooled liquids. Here, we study how spatially correlated dynamic domains evolve with time and compare our results to various experimental and numerical investigations. We find that strong and fragile models yield different results. In particular, the lifetime of dynamic heterogeneity remains constant and roughly equal to the alpha relaxation time in strong models, while it increases more rapidly in fragile models when the glass transition is approached.

1. Introduction

The viscosity of supercooled liquids increases extremely rapidly when the temperature is reduced towards the glass temperature. It is firmly established that this dramatic slowing down is spatially heterogeneous. Local relaxation is widely distributed in time [1] existence of broad stretched relaxations [2], but also in space [3] existence of dynamic heterogeneity [4]. The main physical aspect is that spatial fluctuations of local relaxations become increasingly spatially correlated when temperature decreases. Direct experimental investigations of the time and temperature dependences of the relevant dynamic lengthscales at low temperature are however still missing.

To study dynamic heterogeneity, statistical correlators which probe more than two points in space and time have to be considered [1, 2, 3]. For example, if one wants to study spatial correlations of the local dynamics one has to define a two-point, two-time correlator,

$$C_{2,2}(\vec{r}_i - \vec{r}_j; t) = \langle P_i(0; t) P_j(0; t) \rangle - \langle P_i(0; t) \rangle \langle P_j(0; t) \rangle, \quad (1)$$

where notations are adapted to lattice spin models. In equation (1), (i, j) denote lattice sites, $P_i(0; t)$ quantifies the dynamics at site i between times 0 and t (autocorrelation or persistence functions), and brackets represent ensemble averages. The physical meaning of (1) is clear: given a spontaneous fluctuation of the two-time dynamics at site i , is there a similar fluctuation at site j ? The quantity (1) has now been discussed both theoretically and numerically in some detail [3, 4, 5], generically revealing the existence of a growing spatial range of dynamic correlations in supercooled liquids accompanying an increasingly sluggish dynamics.

^z To whom correspondence should be addressed: berthier@lcvn.univ-montp2.fr

Logically, the next question is then: given spatial structures of the local relaxation between times 0 and t , what will this structure look like, say, between times t and $2t$? In other words [6], how do dynamic heterogeneities evolve with time? This question is in fact simpler to address experimentally because no spatial resolution is needed and different experimental techniques can be devised: NMR [7], solvation dynamics [8], optical [9] and dielectric [10] hole-burning. In statistical terms, one wants to study a four-time correlation function of the general form

$$C_4(t_1; t_w; t_2) = \langle P_i(0; t_1) P_i(t_1 + t_w; t_1 + t_w + t_2) \rangle_i; \quad (2)$$

which correlates dynamics between times 0 and t_1 and between times $t_1 + t_w$ and $t_1 + t_w + t_2$. Again the physical content of (2) is clear [11]: given a dynamic fluctuation at site i between in a certain time interval t_1 , how long does it take for this fluctuation to be washed out? This leads to the general concept of a lifetime, τ_{dh} , for dynamic heterogeneity. While many investigations [1, 2, 7, 8, 10, 12, 13] indicate that τ_{dh} is in fact slaved to the alpha-relaxation time of the liquid, τ_{dh} , photobleaching experiments very close to the glass transition indicate that τ_{dh} may become several orders of magnitude larger than τ_{α} , although in a surprisingly abrupt manner [14].

In this paper we study the lifetime of dynamic heterogeneity in kinetically constrained spin models of supercooled liquids [15]. These models represent schematic coarse-grained models for the glass transition and provide a very efficient tool to study in detail many spatio-temporal aspects related to dynamic heterogeneity such as dynamic lengthscales [16], scaling [17], or decoupling phenomena [18, 19]. They are simple enough that analytical progress can be made and numerical simulations performed on a wide range of lengthscales and timescales, and yet rich enough that direct comparisons to both simulations and experiments can be made.

2. Models

Following previous works [16, 18, 19, 20], we focus on two specific spin facilitated models in one spatial dimension, namely the one-spin facilitated Fredrickson-Andersen (FA) model [21] and the East model [22] that respectively behave as strong and fragile systems [15]. These are probably the simplest models which incorporate the ideas that (i) mobility in supercooled liquids is both highly localized and sparse, as revealed by simulations [12]; (ii) a localized mobility very easily propagates to neighbouring regions, the dynamic facilitation concept. Detailed studies in spatial dimensions larger than one have shown that dimensionality does not play a relevant qualitative role [17, 18, 23], and justify therefore the present one-dimensional studies.

Both models are defined by the same non-interacting Hamiltonian, $H = \sum_i n_i$, expressed in terms of a mobility variable, $n_i = 1$ when site i is mobile, $n_i = 0$ otherwise. Dynamic facilitation is incorporated at the level of the dynamic rules through kinetic constraints. In the FA model, the site i can evolve with Boltzmann probability if at least one of its two neighbours is mobile, $n_{i-1} + n_{i+1} > 0$. In the East model the site i can evolve only if its left neighbour is mobile, $n_{i-1} = 1$.

We have performed numerical simulations of both models using a continuous time Monte Carlo algorithm where all moves are accepted and the time is updated according to the corresponding statistical weight. Simulations have been performed ‘only’ over about 7 decades in time because extensive time averaging is required to accurately measure multi-time correlation functions such as equation (2).

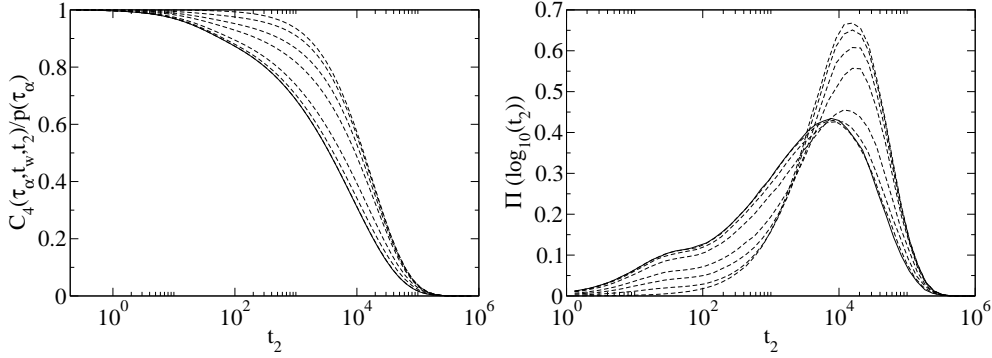


Figure 1. Left: Four-time correlation function $C_4(t_1, t_w, t_2)$ normalized by its $t_2 = 0$ value for various $t_w = 0, 550, 2100, 5200, 20000, 49500$, and 191000 (from right to left) in the FA model at $T = 0.3$. These dashed curves converge at large t_w to the bulk persistence function, $p(t_2)$, shown as a full line. Right: Corresponding logarithmic distributions of relaxation times.

3. Results

3.1. Dynamic filtering

There are several parameters involved in the four-time correlator (2) that need to be appropriately chosen. Since dynamic heterogeneity is more pronounced for times close to it is sensible to restrict $t_1 = 0$ and to study the remaining t_w and t_2 dependences. As a local dynamic correlator we first focus on the persistence function [24], $P_i(0; t) = 1$ if spin i has not flipped in the interval $[0; t]$, $P_i(0; t) = 0$ otherwise. We also define the mean persistence, $p(t) = \langle P_i(t) \rangle$, from which we measure τ via $p(\tau) = e^{-1}$.

In figure 1 (left) we show the t_2 dependence of $C_4(t_1, t_w, t_2)$ for various t_w at $T = 0.3$ in the FA model. We have normalized C_4 by $p(t_2) = e^{-1}$, its value at $t_2 = 0$. By definition, this function describes the persistence function in the interval $[t_w, t_w + t_2]$ of those sites which had not flipped in the interval $[0, t_w]$, and were therefore slower than average. The first term in the correlator (2) plays the role of a dynamic filter [11], selecting a sub-population of sites which have an average dynamics different from the bulk. From earlier works studying the spatial correlator (1), it is known that those sites belong to compact clusters that represent the largest regions of space with no mobility defects at time 0 [16, 17, 23].

Immediately after filtering one expects therefore those slow regions to remain slow, as indeed observed in figure 1 for $t_w = 0$. When t_w increases, this selected population gradually forgets it was initially slow. When $t_w \rightarrow 1$, bulk dynamics is recovered,

$$\frac{C_4(t_1, t_w \rightarrow 1, t_2)}{p(t_2)} \rightarrow p(t_2); \quad (3)$$

as demonstrated by the full line in figure 1. In figure 1 (right) we also show the (logarithmic) distribution of relaxation times corresponding to the functions shown in the left panel, a representation sometimes preferred in experimental works [1]. Both quantities are of course fully equivalent [20]. It is clear from these figures that once a subset of sites has been dynamically selected the remaining relaxation is narrower than the bulk relaxation. In fact all persistence functions shown in figure 1 are well described

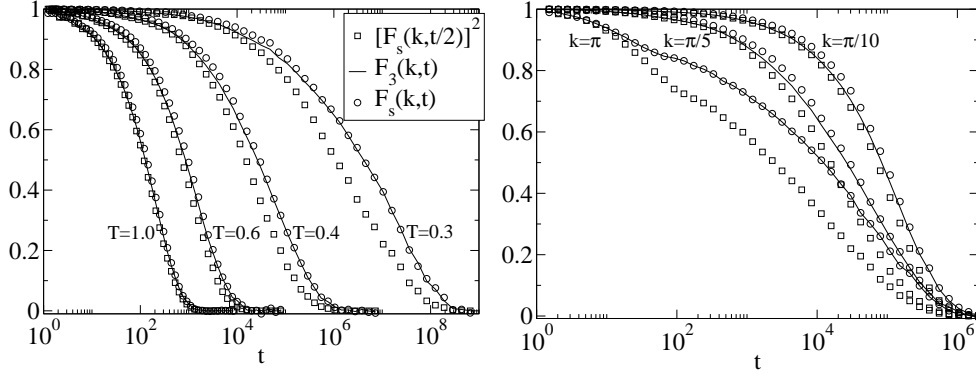


Figure 2. $F_3(k; t)$ and its 'heterogeneous', $F_s(k; t)$, and 'homogeneous', $[F_s(k; t/2)]^2$, limits. Left: East model for fixed $k = \pi/5$ and various temperatures. Right: East model at $T = 0.4$ and various wavevectors.

by stretched exponentials. While $\beta = 1/2$ is observed for the bulk dynamics, one finds 0.83 at $t_w = 0$. Accordingly, distribution of relaxation times progressively broaden when t_w increases. These results are consistent with experimental observations.

In the FA model their interpretation is straightforward. Stretching in this model follows from an exponential distribution of distance between mobility defects [16]. Dynamic clustering implies that this domain distribution is cut-off at small distance. Narrower lengthscale distributions directly imply narrower timescale distributions.

We have also investigated the effect of changing the 'clustering efficiency' [7] which in our case implies changing the duration of the clustering interval, $[0; t_c]$. While bulk distributions are found for $t_c = 1$ (weak clustering) distributions shift to larger times and become very narrow when t_c increases. In the following we work at constant clustering, $t_c = 1$.

3.2. 'Homogeneous' vs. 'heterogeneous' dynamics

The ability to select a sub-ensemble of sites that are slower than average is sometimes taken as a definition of dynamic heterogeneity [7], although lengthscales play no role in this view. That FA and East model display spatially heterogeneous dynamics is well-known, and the results of the previous section are therefore natural.

Another indicator of dynamic heterogeneity has been proposed [11, 25, 26] based on the analysis of the four-time correlation (2). Consider the situation where $t_w = 0$, and $t_1 = t_2 = t/2$. In that case, one studies a 'three-time' correlation [26]

$$F_3(t) = \langle P_i(0; t/2) P_i(t/2; t) \rangle_i \quad (4)$$

Two extreme behaviours can be expected for $F_3(t)$. (i) Dynamics in the intervals $[0; t/2]$ and $[t/2; t]$ are totally uncorrelated, and thus $F_3(t) = \langle p(t/2) \rangle_i^2$. (ii) Dynamics in the two intervals are strongly correlated, in the sense that those regions that survive clustering in $[0; t/2]$ are also those dominating the relaxation in the full interval $[0; t]$. In that case, $F_3(t) = \langle p(t) \rangle_i$. Scenarios (i) and (ii) have been termed 'homogeneous' and 'heterogeneous', respectively, although again lengthscales play no role in the distinction. Clearly, both estimates become equivalent when $p(t)$ decays exponentially.

Of course when studying the persistence function in the FA and East models, scenario (ii) strictly applies by definition, because $P_i(0; t/2) P_i(t/2; t) = P_i(0; t)$. In

real materials, smooother dynamic functions are studied, directly defined from the particles positions instead of a mobility field. Our strategy is therefore to couple probe particles to our mobility field, see Refs. [18, 19] for technical details. From probe molecule displacements, $\mathbf{x}(0;t) = \mathbf{x}(t) - \mathbf{x}(0)$, we define self-intermediate scattering functions, $F_s(k;t) = \langle \cos[\mathbf{k} \cdot \mathbf{x}(0;t)] \rangle$, and the analog of equation (4), $F_3(k;t) = \langle \cos[\mathbf{k} \cdot \mathbf{x}(0;t=2)] \cos[\mathbf{k} \cdot \mathbf{x}(t=2;t)] \rangle$.

Our numerical results are presented in figure 2. Clearly the time dependence of F_3 closely follows the one of $F_s(k;t)$, in agreement with the ‘heterogeneous’ scenario described above. This is consistent with numerical results [26].

In the present approach, this result is a natural consequence of decoupling between structural relaxation and diffusion [18, 19]. At large wavevectors, $k \gg k^*$, corresponding to distances of the order of the lattice spacing, $F_s(k;t)$ is dominated by the time distribution of the first jump of the probe molecule in the interval $[0;t]$, so that $F_s(k;t) \approx p(t) \approx F_3(k;t)$. At large distance, $k < k^*$, Fickian diffusion holds [19], $F_s(k;t) = \exp(-k^2 D_s t)$, and there is no distinction between homogeneous and heterogeneous relaxation. At intermediate wavevectors, $k^* < k < k^*$, the long-time decay of $F_s(k;t)$ is again dominated by the persistence time distribution, because the time scale it takes a molecule to make $2 \approx k$ steps is strongly dominated by the time scale to make the first step [19]. This is just the condition for the heterogeneous scenario to hold, in agreement with figure 2. The characteristic wavevector separating the two regimes, $k^*(T) = 1/\sqrt{D_s \tau_p}$, decreases when temperature decreases, opening a larger heterogeneous window; k^* also sets the upper limit of validity of Fickian diffusion in supercooled liquids [19].

3.3. Lifetime of dynamic heterogeneity

After dynamic filtering it takes some time for filtered distributions to reequilibrate towards the bulk relaxation, cf figure 1. To extract the typical lifetime of dynamic heterogeneity, τ_{dh} , we tried several procedures which all lead to similar results, based on how timescales (time decay of persistence functions or moments of the corresponding distributions) return to their equilibrium values. Following Refs. [13, 18] we also measured the integrated difference between filtered and bulk dynamics, $\int_0^{t_w} dt_2 [C_4(t_w; t_2) - p(t_w) p(t_2)]$. From figure 1, we expect that τ_{dh} goes to 0 on a timescale τ_{dh} . In practice, we define τ_{dh} as $\tau_{dh} = \tau_{dh}(0) = e^{-1}$. In principle, τ_{dh} depends on the filtering time, t_f , and on temperature, T .

We show in figure 3 results at various T but constant filtering time, $t_f = t_f(T)$, in East and FA models. While τ_{dh} is set by τ_p in the FA model (the tiny deviation observed in figure 3 is due to finite T corrections which weaken when T gets lower), this is not true in the East model where τ_{dh} systematically grows faster than τ_p at low T , as emphasized in the inset. Quantitatively a power law relationship, $\tau_{dh} \propto \tau_p^{1+\alpha}$, with $\alpha = 0.06$, is a good description of the data, although alternative fitting formula could probably be used.

In the fragile case, τ_{dh} can therefore be considered as an additional slow timescale characterizing the alpha-relaxation [14], on top of τ_p and $1/D_s$ [18]. The comparative study of FA and East models offers a possible physical interpretation. While both models display stretched relaxations, in the FA model stretching is constant, $\beta = 1/2$, while β increases linearly with T in the East model [20]. Therefore τ_{dh} represents the first moment of a distribution that becomes wider and wider when T decreases. We attribute the small but systematic decoupling between τ_{dh} and τ_p to this broadening.

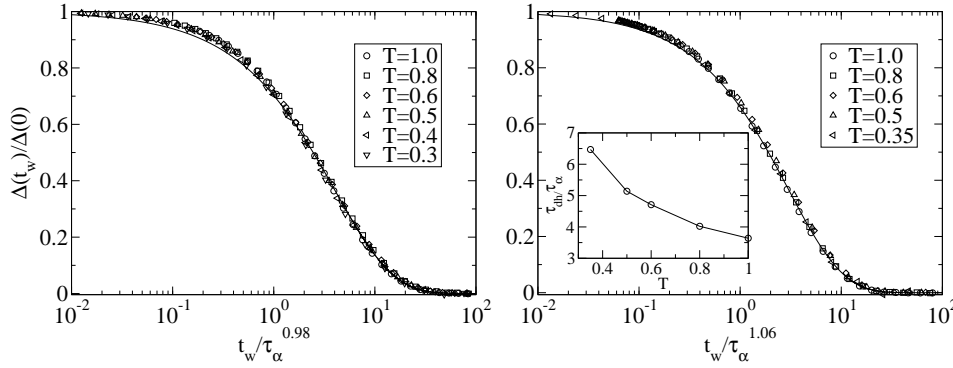


Figure 3. Integrated difference between iterated and bulk dynamics at constant iterating time, $t_l = 1$, and various temperatures in the FA (left) and East (right) models. Times have been rescaled to collapse the data points at various temperatures and extract the lifetime of dynamic heterogeneity, t_{dh} . In the FA model, t_{dh} is set by t_l with tiny corrections that vanish at low T . In the East model, t_{dh} grows faster than t_l , as emphasized in the inset showing the systematic increase of $t_{dh} = t_l$ as T decreases. Mastercurves are fitted by stretched exponentials shown with full lines, $\beta = 0.75$ (left) and $\beta = 0.8$ (right).

Unfortunately this decoupling does not quantitatively account for the results of photobleaching experiments which show that $t_{dh} = t_l$ increases strongly close to T_g [14]. In OTP, while t_l changes by about 1 decade when T is changed from $T_g + 4$ K to $T_g + 1$ K, the ratio $t_{dh} = t_l$ changes by 2 orders of magnitude, so that $t_{dh} = 2 t_l$. This value is much too large to be accounted for by the above results. Presumably, also, t_{dh} does not vary much on such a tiny temperature interval. Therefore, the present results cannot explain the experimental value $t_{dh} = 2 t_l$ without invoking possible non-equilibrium effects due to the proximity of T_g . However we were able to predict instead a smaller, but definitely non-vanishing decoupling between the lifetime of dynamic heterogeneity and the alpha-relaxation time which could be detected in dynamic iterating experiments performed on a sufficiently large temperature window in fragile glass-formers.

References

- [1] M. D. Ediger, *Annu. Rev. Phys. Chem.* **51**, 99 (2000).
- [2] H. Sillescu, *J. Non-Crystalline Solids* **243**, 81 (1999).
- [3] S. C. Glotzer, *J. Non-Crystalline Solids* **274**, 342 (2000).
- [4] C. Bennemann, C. Donati, J. Baschnagel, and S. C. Glotzer, *Nature* **399**, 246 (1999); N. Lacevic, F. W. Starr, T. B. Schröder, and S. C. Glotzer, *J. Chem. Phys.* **119**, 7372 (2003).
- [5] C. Toninelli, M. Wyart, L. Berthier, G. Biroli, and J.-P. Bouchaud, *Phys. Rev. E* **71**, 041505 (2005).
- [6] B. Doliwa and A. Heuer, *J. Non-Crystalline Solids* **307-310**, 32 (2002).
- [7] K. Schmidt-Rohr and H. W. Spiess, *Phys. Rev. Lett.* **66**, 3020 (1992); R. Bohmer, G. Diezemann, G. Hinze, and H. Sillescu, *J. Chem. Phys.* **108**, 890 (1998).
- [8] M. Yang and R. Richert, *J. Chem. Phys.* **115**, 2676 (2001).
- [9] M. D. Ediger, *J. Chem. Phys.* **103**, 752 (1995).
- [10] B. Schiener, R. Bohmer, A. Loidl, and R. V. Chamberlin, *Science* **274**, 752 (1996).
- [11] A. Heuer, *Phys. Rev. E* **56**, 730 (1997).
- [12] D. N. Perera and P. Harrowell, *J. Chem. Phys.* **111**, 5441 (1999).
- [13] E. Flenner and G. Szamel, *Phys. Rev. E* **70**, 052501 (2004).
- [14] C.-Y. Wang and M. D. Ediger, *J. Phys. Chem. B* **103**, 4177 (1999).
- [15] F. Ritort and P. Sollich, *Adv. Phys.* **52**, 219 (2003).

- [16] J.P. Garrahan and D. Chandler, Phys. Rev. Lett. 89, 035704 (2002).
- [17] S. Whitelam, L. Berthier, and J.P. Garrahan, Phys. Rev. Lett. 92, 185705 (2004); Phys. Rev. E 71, 026128 (2005).
- [18] Y. Jung, J.P. Garrahan and D. Chandler, Phys. Rev. 69, 061205 (2004); preprint cond-mat/0504535.
- [19] L. Berthier, D. Chandler, and J.P. Garrahan, Europhys. Lett. 69, 230 (2005).
- [20] L. Berthier and J.P. Garrahan, J. Chem. Phys. 119, 4367 (2003); Phys. Rev. E 68, 041201 (2003).
- [21] G.H. Fredrickson and H.C. Andersen, Phys. Rev. 53, 1244 (1984).
- [22] J. Jackle and S. Eisinger, Z. Phys. B 84, 115 (1991).
- [23] L. Berthier and J.P. Garrahan, J. Phys. Chem. 109, 3578 (2005).
- [24] A. Heuer, U. Tracht, and H.W. Spiess, J. Chem. Phys. 107, 3813 (1997).
- [25] A. Heuer and K. O'Kun, J. Chem. Phys. 106, 6176 (1997).
- [26] B. Doliwa and A. Heuer, Phys. Rev. Lett. 80, 4915 (1998).